

Theoretical Study of Ternary CoSP Semiconductor: a Candidate for Photovoltaic Applications

Abdesalem Houari* and Fares Benissad

Theoretical Physics Laboratory, Department of Physics,

University of Bejaia, Bejaia, Algeria

(Dated: March 24, 2020)

Abstract

The electronic structure of pyrite-type cobalt phosphosulfide (CoSP) has been studied using density-functional theory. The calculated band structure reveals the non-magnetic semiconducting character of the compound. The electronic structure is described through the electronic band structure and the densities of states. A band gap of 1.14 eV has been computed within standard GGA, a value which is enhanced using hybrid functional. It separates the upper part of the valence band dominated by Co- $3d-t_{2g}$ states from the lower part of the conduction band made exclusively of Co- $3d-e_g$, above of which lie S- $3p$ and P- $3p$ ones. The obtained values are suitable for applications in solar cells, according to Shockley-Queisser theory of light to electric conversion efficiency. The origin of the larger CoSP band gap, with respect to the one of the promising FeS₂ compound, is explained and the chemical bonding properties are addressed. A comparative picture is established where several similarities have been found, suggesting that CoSP could be for a great practical interest in photovoltaics.

*corresponding author: abdeslam.houari@univ-bejaia.dz

Contents

I. Introduction	2
II. Computational Method	4
III. Results and Discussions	5
IV. Summary and Conclusion	9
Acknowledgments	10
References	10

I. INTRODUCTION

Pyrite-type iron disulfide (FeS_2) is considered as a promising material for photovoltaic applications [1–3]. The non toxicity and the abundance on the earth surface, as a mineral [4–6], make this compound very interesting for practical usage and technology. Another important advantage is its high optical absorption [7], which is one of the key requirement in solar cell applications. The role of surface states, defects and non-stoichiometry with respect to their implications on the photovoltaic performance have been recently addressed, by means of *ab-initio* methods [8–10]. Moreover, FeS_2 has attracted much interests in other areas. For instance, it has been investigated in recent years as a hydrogen evolution reaction (HER)catalyst[11, 12]. It was also found that it could be a candidate for thermoelectricity, due to it’s good thermopower, compared to other materials intended for practical use [13, 14]. The efficiency and the performance of a thermoelectric material is characterized by its figure of merit (zT) which is proportional to the square of the thermopower (S^2).

For photovoltaic applications, however, an important handicap for single junction cells applications comes from its gap magnitude (experiments give 0.9 eV) which is smaller than the optimal value predicted by Shockley-Queisser theory [15]. Recently, tabulated values for the maximum efficiency of light to electric power conversion have been provided as function of the solar cell band gap [16]. The highest one of $\sim 33.16\%$ is reached at 1.34 eV of this latter, and conversion efficiencies above 30% can be obtained for band gaps between 1 eV and

1.7 eV. From this, the FeS₂ one is 0.44 eV smaller than the optimal one. In this context, a lot of efforts have been devoted to increase its gap and to improve its other physical properties[17]. A well known scheme for tuning electronic properties of semiconductors, such as band gap, is alloying via substitution[18].

In pyrite-type transition metal disulfides TS₂ (T=Mn, Fe, Co and Ni), it's rather the metallic substitution which is mostly considered and commonly explored [19]. Particularly, a large variety is reported in literature about iron pyrite giving rise to Fe_{1-x}T_xS₂ alloys with different properties (see [17, 19, 20] and references therein). On the other side, however, much less attention has been given to non-metallic *i.e.* sulfur substitution. Nevertheless, alloying with oxygen to form FeS_{2-x}O_x has been recently reported [21]. By replacing about 10% of the sulfur atoms, a band gap in a range from about 1.2 eV to 1.3 eV has been obtained. In addition to some few investigations in electrocatalysis [22, 23], there is no much reports dealing with light elements, such as first and second row elements (C, O, Al, Si, P ..etc), replacing sulfur.

In view of the growing interest to enhance FeS₂ properties, it appears highly desirable to find new candidates with similar interest and suitable properties for photovoltaics and thermoelectrics. Starting from the neighboring isostructural cobalt disulfide CoS₂, a hardly known semiconductor was identified in early 1960s by replacing one sulfur atom with one phosphorus *i.e.* the cobalt mono-phosphosulfide Co₁S₁P₁ [24]. In recent experimental study, Acevedo *et al.* [25] have confirmed that this compound remains in the pyrite crystal structure, and could be for a great interest as high-performance catalyst for hydrogen production. According to the authors, its crystal structure can be described by Co³⁺ octahedra and *S-P* dumbbells, with a homogeneous distribution of P²⁻ and S¹⁻ atoms. Having one electron less than CoS₂, ternary CoSP is isoelectronic to FeS₂, which is consistent with the observed semiconducting character. The reported lattice constant ($a=5.422\text{\AA}$) [24] is almost equal to the FeS₂ one ($a=5.415\text{\AA}$), while being smaller than the CoS₂ corresponding constant ($a=5.538\text{\AA}$). Except these mentioned structural data, we did not find much works in literature on this cobalt phosphosulfide compound. Its physical properties (electronic, optical ..etc) remain unexplored both experimentally as well as theoretically.

To study correctly the optical properties (usually more difficult within standard DFT and need to go beyond one particle approximation), a complete and clear picture of the electronic structure is necessary beforehand. That is, we restrict our present study to the

electronic properties of CoSP compound, through the computation of band structure and densities of states. Further insights are given by comparing the results with well established ones of FeS₂.

The paper is organized as follows: In Sec. II, we describe the theoretical method and the computational details. In Sec. III we present our results and a summary is finally given in Sec. IV

II. COMPUTATIONAL METHOD

The *ab-initio* calculations are carried out in the framework of density-functional theory (DFT)[26, 27]. The electronic properties (band structure and densities of states), have been obtained with the Projector Augmented Wave (PAW) method[29] as implemented originally in the CP-PAW code. The PAW method is an *all-electron* electronic structure method, where the full wave functions including their nodal structure are properly defined. The PAW formalism combine and generalize ideas of both pseudopotentials (USPP)[30] and the linearized augmented-plane-wave (LAPW) method [31]. The method recovers the missing link between both approaches. Compared to the former, PAW is more rigorous, and can be made exact by converging series expansions. A thorough description of the method can be found in the original paper by P. E. Blöchl [29].

The exchange-correlation effects are accounted within the generalized gradient approximation (GGA) of Perdew-Burke-Ernzerhof [28]. Moreover, we also performed calculations using the hybrid PBE0r functional, which replaces a fraction of the exchange term of the PBE functional with the exact Fock-term[32, 33]. Unlike in PBE0[34], it uses the idea of range separated (screened) hybrid functional[35], where the slowly decaying long-range part of the Fock exchange interaction is replaced by the corresponding part of the PBE counterpart. The PBE0r functional has been developed by Blöchl *et al.* [36, 37], where the range separation correction is restricted to the onsite interactions in a local orbital basis. The scaling of the onsite terms combined with the truncation of off-site terms approximates the screening of the interaction in the exchange term in the spirit of the random phase approximation. The double counting term or the removal of the GGA exchange is done consistent with choice of the screened U-tensor used in the Fock term. [36]. The mixing parameter for the exchange can be chosen independent for each atom. So far, the best agreement with

spectral properties has been obtained with a mixing factor close to $\frac{1}{8}$, and PBE0r functional has shown to be accurate for transition-metal oxides with a partially filled d-shell [38].

CP-PAW employs the framework of Car-Parrinello *ab-initio* molecular dynamics (AIMD)[39] for the optimization of wave functions and atomic structure. It is based on a fictitious Lagrangian from which a set of Euler-Lagrange type equations of motion are derived for the electronic wavefunctions as well as for the atomic positions. In the Car-Parrinello method, the electronic wavefunctions and atomic positions are treated on an equal footing, and the groundstate is simulated by applying friction.

For the augmentation, we used a $s^1p^1d^1$ set of projector functions for all atoms, where the superscripts denotes the number of projector functions angular momentum channel. The convergence of the total energy minimization is reached when the difference between two successive iterations is less than 10^{-5} Hartree (also known as the self-consistency convergence criterion). On the other hand, the convergence of the total energy versus two important parameters, which are the plane wave cutoff (wavefunction and density) and the number of k -points in the Brillouin-zone, has been also obtained carefully. For the former, several increasing cutoff values (30, 40, 60 up to 70 Ry) have been considered. With values higher than 40 Ry, the variation in the computed total energy is less 10^{-4} Hartree which is always considered as a very good accuracy in the field of DFT calculations. The Brillouin-zone integration has been performed with the linear tetrahedron method[40, 41] and the so-called Blöchl corrections[42]. As for plane wave cutoff, in order to ensure the convergence of the total energy versus the k -points sampling, the calculations have been carried out with increasing grids (from $4 \times 4 \times 4$ up to $7 \times 7 \times 7$). With a $6 \times 6 \times 6$ mesh, leading to 112 k -points in the irreducible Brillouin-zone, an accuracy of 10^{-4} Hartree has been reached. All structural parameters (lattice constant and atomic positions) have been optimized.

III. RESULTS AND DISCUSSIONS

We address here the structural and electronic properties of the cobalt phosphosulfide CoSP. In the following, we give an exhaustive discussion of the electronic band structure and densities of states (DOS). Simultaneously, differences and similarities with the well established electronic structure of FeS₂ are highlighted.

The calculated lattice constant and bond lengths (Co-S, Co-P and S-P) within GGA are

TABLE I: Calculated lattice constant (a) and bond lengths (in Å) within GGA for CoSP. For sake of comparison, the corresponding data for iron and cobalt disulfides (FeS₂ and CoS₂) are shown. Experimental data[25, 43] are given in parentheses.

	$a[\text{Å}]$	Bond lengths ([Å])
CoSP	5.411 (5.422)	$d_{\text{Co-S}}=2.278$ $d_{\text{Co-P}}=2.266$ $d_{\text{S-P}}=2.106$
FeS ₂	5.405 (5.416)	$d_{\text{Fe-S}}=2.263$ $d_{\text{S-S}}=2.160$
CoS ₂	5.489 (5.538)	$d_{\text{Co-S}}=2.310$ $d_{\text{S-S}}=2.101$

given in Table I, in addition to the calculated corresponding data of FeS₂ and CoS₂. The latter, as well as the experimental data shown between parentheses, are included for sake of comparison. The calculated values are in very good agreement with experimental ones. The results obtained with hybrid functional are very close, (only 0.1% larger) and consequently have been omitted in the table. As it can be noticed, the Co-S(P) bond lengths lie between the corresponding ones of the pure compounds, being much closer to Fe-S than to Co-S. This is consistent with the lattice constant values of the three compounds. On the other hand, however, the non-metallic S-P dumbbell distance in CoSP is almost equal to the S-S one in CoS₂. It is relatively shorter than the corresponding one in FeS₂, and this will have very important effects, especially on the gap property.

It has been shown that a very small change of the S-S bond length in FeS₂ could influence drastically the band gap magnitude (and even its nature) [10]. Only small shortening could lead to a substantial increase of the band gap. In view of the structural results (see Table I), we expect an enhanced band gap in CoSP compared to FeS₂. As a matter of fact, this is confirmed in a first step within GGA framework. The plots of electronic band structure along the first Brillouin zone high-symmetry points of the simple cubic unit cell is illustrated in Fig.1. The filled (core and valence) bands are shown in black color and the empty conduction bands are shown in blue color. The maximum of the former VB_{MAX} is separated by a gap $E_g \sim 1.14$ eV from the minimum of the latter CB_{MIN}. The individual contribution of the atomic species cobalt, sulfur and phosphorus to the bands occupation will appear in the next paragraph through the DOS plots.

From Fig.1 we notice that the CoSP band gap is an indirect one. This latter feature

is common to FeS₂ compound, as well as the whole trend of the bands distribution which seems very similar (see references [19, 46]). These similarities could be attributed to the fact that both compounds are isostructural, but more important are isoelectronic i.e. they have the same valence configuration. The extra electron brought by cobalt with respect to iron, is lost when one sulfur is replaced by phosphorus. Finally, we mention that taking in account the spin polarization results in a zero magnetic moment of the unit cell, as well as for individual atomic species, leading to non magnetic semiconductor.

The properties of FeS₂ are well established both experimentally and theoretically. We just recall that it's a semiconductor, with an indirect band gap and most of the experimental measurements give ~ 0.9 eV [1, 44, 45] (a good account of the computed and measured FeS₂ gap is reported in reference [46]). In a previous work on Fe(Mn, Ni)S₂ alloys [19], our GGA calculations gave $E_g \sim 0.35$ eV, much smaller than experimental value. The filled Fe- t_{2g} states form a narrow sub-bands in the top of the valence band, whereas Fe- e_g ones in the bottom of the conduction band are empty. An important detail to mention, however, is that the lowest edge of the conduction band has an S- p character.

The main difference in CoSP concerns this latter (CB_{MIN} in Fig.1) which is made of Co- e_g type making the gap exclusively between cobalt metallic states. As pointed out above, the short bond length of S-P dumbbell (compared to S-S one in FeS₂), shifts up the p -states of sulfur and phosphorus in the conduction band to higher energies above the Co- e_g ones, and consequently leads to a wider band gap. This mechanism proposed first on the basis of DFT calculations, has been exploited in recent experiments where an improved FeS₂ gap was achieved through oxygen substitution (oxygen is isoelectronic of sulfur)[47].

This underestimation of band gaps in solids is a well known failure of the Kohn-Sham DFT framework [48]. One way to cure this discrepancy is the use of hybrid functional. With a fraction of 10% of (exact) Fock exchange, we have reproduced the correct value for FeS₂. Following the same procedure here i.e. assuming the same weight of the Fock term, a gap of $E_g \sim 1.65$ eV has been calculated. Therefore, we expect the experimental gap to be around the latter value, with the GGA's value being a lower limit (~ 1.14 eV). Regarding this gap value property in particular, the compound could attract a great interest for photovoltaic single-junction in solar-cell energy production. As pointed out in the introduction, according to Shockley-Queisser theory [15, 16], the range between 1.0 eV and 1.7 eV leads to the closest values of the threshold efficiency (obtained for $E_g \sim 1.4$ eV), and thus our CoSP predicted

ones (either with GGA or hybrid functional) lies in this interval.

The electronic densities of states (DOS) are shown in Fig.2. Since phosphorus and sulfur are neighboring atomic species (i.e, P has one electron less than S), their states lie in the same energy window. The bottom of the valence band constituted mainly by s -states of P and S are not shown here (the corresponding bands are, however, visible between -9 and -15 eV in Fig.1). As shown in the upper panel, the non-metallic contribution (i.e. S and P states) dominate from -7 eV to -4 eV, whereas a large part of cobalt states are concentrated as one block in narrow energy window between -2 eV and -0.8 eV. In addition, the metallic states still contribute with a large part, with a small mixture of S and P ones in the middle region from -3 eV to -2 eV. In the lower panel of Fig.2, the crystal field splitting of cobalt d -states to its t_{2g} and e_g contributions is illustrated , where a quite clear separation between them is noticeable. The former is almost exclusively located in the narrow energy window of the top of the valence band with a small admixture of e_g states. These latter are in one hand spread in the middle between -5 eV and -2 eV, and on the other hand dominate the bottom of the empty conduction bands around +2 eV. Thus, the cobalt t_{2g} sub-bands are fully occupied, whereas e_g ones are only half occupied.

The behavior of the chemical bonding in CoSP compound is described in Fig.3 with the help of a sketch in the form of a molecular orbitals diagram. It has to be mentioned that this is just a qualitative illustration of the average trend and not a quantitative study of the chemical bonding of the system. It can be decomposed into three main different regions. In the lower part, from -7 eV to -4 eV, a clear hybridization between p_z -type states of sulfur and phosphorus is involved, leading to a strong S(P)- $pp\sigma$ bond. In the middle of the valence band (from -4 eV to -1 eV), we find the weaker S(P)- $pp\pi$ bond and its counter part antibonding S(P)- $pp\pi^*$ one. This latter is mainly mixed with a small fraction of bonding Co- e_g states. An important non-bonding block of Co- t_{2g} orbitals dominate the top of the valence band from -1.5 eV until the gap. Finally, an important antibonding Co- e_g states occupy the lower part of the conduction bands up to +3 eV. They coexist with the antibonding S(P)- $pp\sigma^*$ which are spread to higher energies and dominate the region above +3 eV.

Finally, we mention that except the improved value of the gap, the behavior and the features of the band structure, the densities of states and the chemical bonding obtained with the hybrid functional are almost identical to those obtained with GGA. Therefore, both frameworks give the same description of the compound and so the same discussion holds.

Before summarizing, we want to point out an important point related to the optical properties, already mentioned in $\text{FeS}_{2-x}\text{O}_x$ study [47]. In this latter, the optical absorption comes mainly from transitions between metallic states (from t_{2g} to e_g states). It's found that the insertion of oxygen replacing sulfur, reducing the local symmetry of Fe- e_g bands, improves the whole absorption. Such situation is almost identical here with CoSP, and consequently we expect similar interesting optical properties (high optical absorption and suitable band gap for efficient light-electricity conversion). A study dedicated to these latter is in progress.

IV. SUMMARY AND CONCLUSION

To conclude, we explored using first-principles calculations, the electronic structure and chemical bonding of CoSP semiconductor crystallizing in pyrite type crystal structure.

Being isostructural and isoelectronic to FeS_2 , interesting optical properties like those of this latter are expected. CoSP compound has been found to have a larger band gap. It is estimated to ~ 1.14 eV, within GGA and a value of ~ 1.65 eV is obtained using hybrid functional. These values are highly suitable for practical usage in solar cell as predicted by Shockley-Queisser theory, since they belong to the highest range of light to electric conversion efficiencies. Therefore, CoSP could be considered as a promising compound for photovoltaic applications, and experimental data are called for to confirm our predictions.

The whole trend of the electronic structure is similar to FeS_2 , where the effect of the crystal field on the cobalt $3d$ -states is clearly visible. The important hybridization of the p_z -states within S-P dumbbell gives rise to a strong σ -bond in the bottom of the valence band, largely splitted from its counter part σ^* -antibond in the conduction band. Like in iron pyrite, the cobalt t_{2g} states form a narrow non-bonding block dominating the top of the valence band.

The most important and noticeable feature in CoSP concern the lowest edge of the conduction band which is of Co- e_g character and the larger value of the gap. This feature is attributed to the S-P bond length which is found to play a crucial role. Its shorter magnitude (compared to S-S one FeS_2) shifts up the S(P)- p_z states to higher energy. This results in a wider band gap which now separate exclusively metallic states i.e, Co- t_{2g} states (VB_{MAX}) from the Co- e_g ones (CB_{MIN}).

Acknowledgments

A.H. gratefully acknowledges Prof. Dr. Peter E. Blöchl from Clausthal University of Technology (Germany) for several stays spent in his group and for fruitful scientific discussions. In particular for having provided us the detailed description of their exchange-correlations functional PBE0r of section II (Computational Method).

- [1] A. Ennaoui, S. Fiechter, Ch. Pettenkofer, N. Alonso-Vante, K. Büker, M. Bronold, Ch. Höpfner and H. Tributsch, *Sol. Ener. Mat. and Sol. Cells* **29**, 289, (1993)
- [2] C. Wadia, A. P. Alivisatos and D. M. Kammen, *Envir. Scie. & Techn* **43**, 2072(2009)
- [3] M. Caban-Acevedo, N. S. Kaiser, C. R. English, D. Liang, B. J. Thompson, H. Chen, K. Czech, J. Wright, R. Hamers and S. Jin, *J. Am. Chem. Soc.* **136** 17163, (2014)
- [4] A. Ennaoui, S. Fiechter, W. Jaegermann and H. Tributsch, *Jour. Electrochem. Soc.* **133**, 97 (1986)
- [5] M. Birkholz, S. Fiechter, A. Hartmann and H. Tributsch, *Phys. Rev. B* **43**, 11926 (1991)
- [6] R. Murphy and D. R. Strongin, *Sur. Scie. Rep.* **64**, 1 (2009)
- [7] I. J. Ferrer, D. M. Nevskaiia, C. de las Heras and C. Sanchez, *Sol. State. Com.* **74**, 913 (1990)
- [8] R. Sun, M. K. Chan and G. Ceder, *Phys. Rev. B* **83**, 235311 (2011)
- [9] R. Sun, M. K. Chan, S. Kang and G. Ceder, *Phys. Rev. B* **84**, 035212 (2011)
- [10] V. Eyert, K-H. Höck, S. Fiechter and H. Tributsch, *Phys. Rev. B* **57**, 6350 (1998)
- [11] D. Kong, J. Cha, H. Wang, H. Lee, and Y. Cui, *Energy Environ. Sci.* **6**, 3553 (2013)
- [12] M. Faber, M. Lukowski, Mark Q. Ding, N. Kaiser, and S. Jin, *Song, J. Phys. Chem. C* **118**, 21347 (2014)
- [13] T. M. Bither, R. J. Bouchard, W. H. Cloud, P. Donohue and W. J. Siemons, *Inorg. Chem.* **7**, 2208 (1968)
- [14] V. K. Gudelli, V. Kanchana, S. Appalakondaiah, G. Vaitheeswarana and M. C. Valsakumar, *J. Phys. Chem. C* **117**, 21120 (2013)
- [15] W. Shockley and H. J. Queisser, *J. Appl. Phys.* **32**, 510 (1961)
- [16] S. Ruhle, *Sol. Energy* **130**, 139 (2016)
- [17] R. Sun and G. Ceder, *Phys. Rev. B* **84**, 245211 (2011)

- [18] S. H. Wei and A. Zunger, *J. Appl. Phys.* **78**, 3846 (1995)
- [19] A. Houari and P. E. Blöchl, *J. Phys. Cond. Mat.* **30**, 305501 (2018)
- [20] S. Khalid, M. A. Malik, D. Lewis, P. Kevin, E. Ahmed, Y. Khan, and P. O'Brien, *J. Mater. Chem. C* **3**, 12068 (2015)
- [21] R. Wu, M. Law, J. Hu and Y. Zhang, Google. Patents, US PATENT **9.450,120-B2**, (2016)
- [22] Z. Wu, X. Li, W. Liu, Y. Zhong, Q. Gan, X. Li and H. Wang, *ACS Catal.* **7**, 4026 (2017)
- [23] J. Li, Z. Xia, X. Zhou, Y. Qin, Y. Ma and Y. Qu, *Nano. Research* **10**,814 (2017)
- [24] F. Hulliger, *Nature* **198**, 382 (1963)
- [25] M. Caban-Acevedo, M. Stone, J. R. Schmidt and J. G. Thomas, *Nature Materials* **14**, 1245 (2015)
- [26] P. Hohenberg and W. Kohn, *Phys. Rev.* **136**, B864 (1964).
- [27] W. Kohn and L. J. Sham, *Phys. Rev.* **140**, A1133 (1965).
- [28] J. P. Perdew, K. Burke and M. Ernzerhof, *Phys. Rev. Lett.* **77**, 3865 (1996); *Phys. Rev. Lett.* **78**, 1396(E) (1997).
- [29] P. E. Blöchl, *Phys. Rev. B* **50**, 17953 (1994).
- [30] D. Vanderbilt *Phys. Rev. B* **41**, 7892(R) (1990)
- [31] O. K. Andersen *Phys. Rev. B* **12**, 3060 (1975)
- [32] A. D. Becke, *J. Chem. Phys.* **98**, 1372 (1993)
- [33] J. P. Perdew, M. Ernzerhof and K. Burke, *J. Chem. Phys.* **105**, 9982 (1996)
- [34] C. Adamo and V. Barone, *J. Chem. Phys.* **110**, 6158 (1999)
- [35] J. Heyd, G.E. Scuseria and M. Ernzerhof, *J. Chem. Phys.* **118**, 8207 (2003)
- [36] P. E. Blöchl, C. F. J. Walther and T. Pruschke *Phys. Rev. B* **84**, 205101 (2011).
- [37] P. E. Blöchl, Th. Pruschke and M. Potthoff *Phys. Rev. B* **88**, 205139 (2013).
- [38] M. Sotoudeh, S. Rajpurohit, P. E. Blöchl, D. Mierwald, J. Norpoth, V. Roddatis, St. Mildner, B. Kressdorf, B. Iffland and C. Jooss *Phys. Rev. B* **95**, 235150 (2017).
- [39] R. Car and M. Parrinello, *Phys. Rev. Lett.* **55**, 2471 (1985)
- [40] O. Jepsen and O.K. Andersen, *Sol. St. Commun.* **9**, 1763 (1971)
- [41] G. Lehmann and M. Taut, *Phys. Stat. Sol. B* **54**, 469 (1972)
- [42] P. E. Blöchl, O. Jepsen O. K. and Andersen, *Phys. Rev. B* **49**, 16223 (1994)
- [43] A. Fujimori, K. Mamiya, T. Mizokawa, T. Miyadai, T. Sekiguchi, H. Takahashi, N. Môri and S. Suga, *Phys. Rev. B* **54**, 16329 (1996)

- [44] A. Schlegel and P. Wachter, *J. Phys. C: Solid State Physics* **9**, 3363 (1976)
- [45] E. K. Li, K. H. Johnson, D. E. Eastman and J. L. Freeouf, *Phys. Rev. Lett.* **32**, 470 (1974)
- [46] D. Banjara, Y. Malozovski, L. Franklin and D. Bagayoko, *AIP. Advances* **8**, 025212 (2018)
- [47] J. Hu, Y. Zhang, M. Law and R. Wu, *J. Am. Chem. Soc.* **134**, 13216 (2012)
- [48] J. P. Perdew, W. Yang, K. Burke, Z. Yang, E. K. Gross, M. Scheffler, G. E. Scuseria, T. Henderson, I. Zhang, A. Ruzsinszky, H. Peng, J. Sun, E. Trushin and Görling, Andreas, *Proc. Nat. Aca. Sci.* **114**, 2801 (2017)

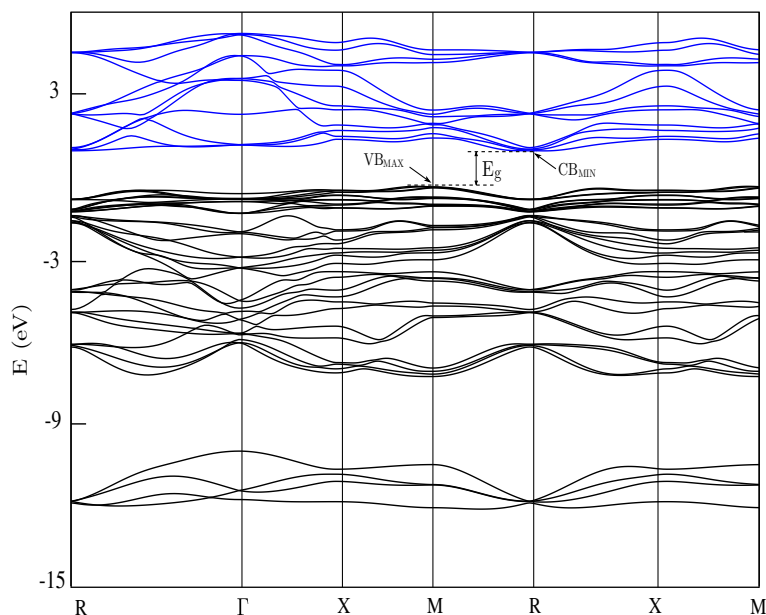


FIG. 1: (Color online) Electronic band structure (eV) of CoSP along selected high symmetry lines of the 1st Brillouin zone of the simple cubic lattice. The filled states (core and valence bands) are drawn in black color, whereas the empty states (conduction bands) in blue. The valence band maximum (VB_{MAX}) and conduction band minimum (CB_{MIN}) are separated by a band gap E_g .

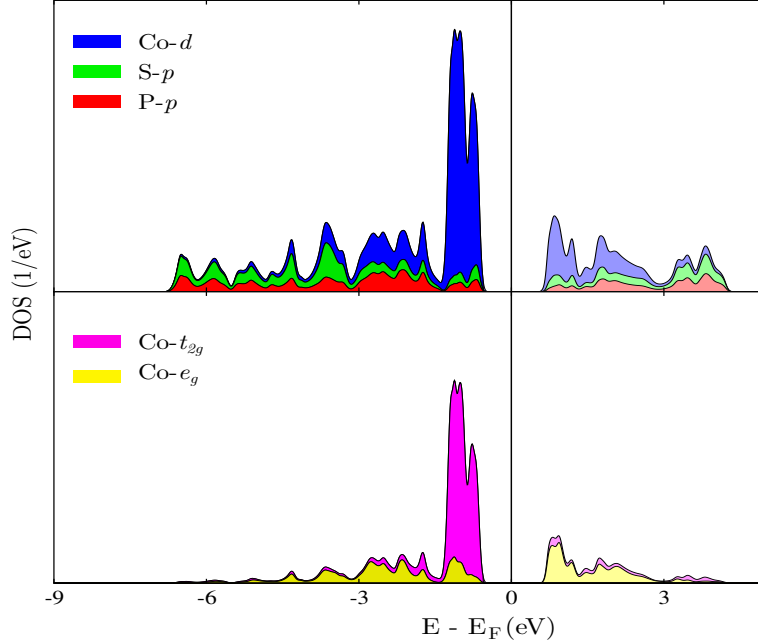


FIG. 2: (Color online) Density of states (DOS) of CoSP, where the energy axis origin is set to the Fermi level E_F . The upper panel: atomic site projected DOS are drawn with distinct color as follow: Co- d , S- p and P- p states are represented by blue, green and red colors respectively. The lower panel: Co- d states splitted into t_{2g} (magenta) and e_g (yellow) contributions. To illustrate well the atomic species contributions individually, each density is drawn in the top of another.

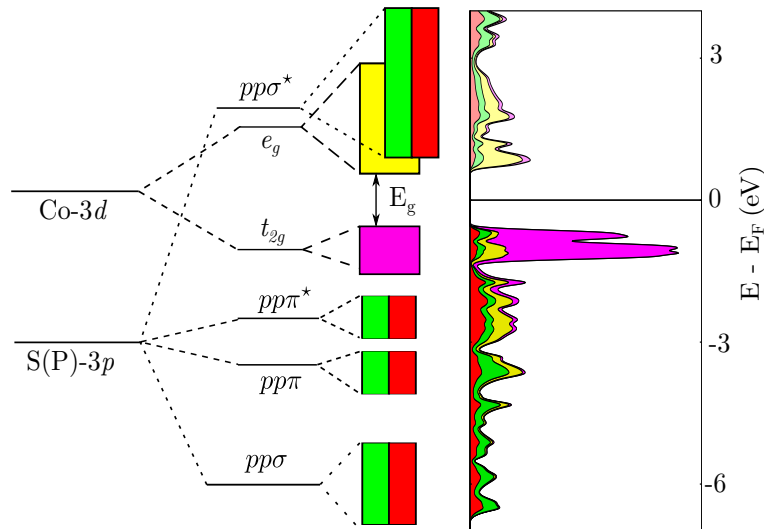


FIG. 3: (Color online) Qualitative illustration of the chemical bonding behavior in CoSP, through the density of states (DOS) plots. A sketch in the form of a molecular orbitals diagram showing the main bonding characters of the system.